A Laboratory Model to Evaluate Cutout Resistance of Implants for Pertrochanteric Fracture Fixation

Mark B. Sommers, MS, Christoph Roth, MS,† H. Hall, MS,† Benjamin C. C. Kam, MD,‡ Larry W. Ehmke, MS,* James C. Krieg, MD,* Steven M. Madey, MD,* and Michael Bottlang, PhD**

Objectives: To establish a laboratory model of implant cutout, which can evaluate the effect of implant design on cutout resistance in a clinically realistic "worst case" scenario.

Setting: Orthopaedic biomechanics laboratory.

Design: Implant cutout was simulated in an unstable pertrochanteric fracture model, which accounted for dynamic loading, osteoporotic bone, and a defined implant offset. For model characterization, lag screw cutout was simulated in human cadaveric specimens and in polyurethane foam surrogates. Subsequently, foam surrogates were used to determine differences in cutout resistance between 2 common lag screws (dynamic hip screw, Gamma) and 2 novel blade-type implant designs (dynamic helical hip system, trochanteric fixation nail).

Main Outcome Measures: Implant migration was continuously recorded with a spatial motion tracking system as a function of the applied loading cycles. In addition, the total number of loading cycles to cutout failure was determined for specific load amplitudes.

Results: Implant migration in polyurethane surrogates closely correlated with that in cadaveric specimens, but yielded higher reproducibility and consistent cutout failure. The cutout model was able to delineate significant differences in cutout resistance between specific implant designs. At any of 4 load amplitudes (0.8 kN, 1.0 kN, 1.2 kN, 1.4 kN) dynamic hip screw lag screws failed earliest. The gamma nail lag screw could sustain significantly more loading cycles than the dynamic hip screw. Of all implants, trochanteric fixation nail implants demonstrated the highest cutout resistance.

Conclusions: Implant design can significantly affect the fixation strength and cutout resistance of implants for pertrochanteric fracture fixation. The novel cutout model can predict differences in cutout resistance between distinct implant designs.

Accepted for publication January 13, 2004.

From the *Biomechanics Laboratory, Legacy Clinical Research & Technology Center, Portland, OR, †Synthes USA, West Chester, PA, and ‡Department of Orthopaedics & Rehabilitation, Oregon Health & Science University, Portland, OR.

Supported in part by Synthes USA, West Chester, PA.

The devices that are the subject of this manuscript are FDA approved.

Reprints: Michael Bottlang, PhD, Biomechanics Laboratory, Legacy Clinical Research & Technology Center, 1225 NE 2nd Avenue, Portland, OR 97232 (e-mail: mbottlan@lhs.org).

Key Words: hip, cutout model, pertrochanteric fracture, lag screw, fixation

(*J Orthop Trauma* 2004;18:361–368)

Each year, over 250,000 hip fractures occur in the United States.[1] The preferred treatment option for pertrochanteric fractures is the use of dynamic lag screws, either as side-plate devices or as part of intramedullary nail constructs. This technique can yield a success rate of over 95%.[2–4] However, in the presence of predisposing factors such as osteoporosis,[5] unstable fractures,[6,7] poor reduction,[6] and inadequate lag screw placement,[6,8–10] complication rates can dramatically increase to over 20%.[8,11,12] The most common failure mechanism is migration of the femoral head into varus and retroversion, and subsequent extrusion, or so-called cutout, of the lag screw through the femoral head.[7]

In cases of posteromedial comminution and poor bone quality, stable fixation is difficult to achieve and maintain. In these instances, the ability of the implant to resist cutout under dynamic loading becomes of utmost importance. A host of clinical and laboratory studies have attempted to determine which implant designs exhibit the lowest incidence of cutout failure. However, clinical studies have consistently failed to find significant differences between implant designs[3,4,13,14] because the incidence of implant-related cutout is masked by the high variability in bone quality, fracture pattern, quality of reduction, and implant placement. Laboratory studies on cadaveric specimens enabled cutout simulation in controlled unstable pertrochanteric fracture models with reproducible lag screw placement under defined loading conditions.[10,15–21] However, none of these studies has combined adverse factors to simulate a scenario in which cutout is most likely to occur in a clinical setting, such as, in the presence of dynamic loading, osteoporotic bone, unstable fractures, and nonideal implant placement.

This study introduces a laboratory model to evaluate the effectiveness of implants of different design to resist migration and cutout failure under such critical operating conditions. After model validation by direct correlation to human cadaveric specimens, 2 common lag screws and 2 novel blade-type im-

plants were tested in surrogate specimens to determine differences in cutout resistance.

MATERIALS AND METHODS

Cutout Model

Surrogate specimens of the femoral head and neck with defined geometry (50-mm diameter head) and material properties (36 MPa compressive modulus) were custom-made of cellular polyurethane foam (Pacific Research Inc., Vashon, WA) to resemble osteoporotic cancellous bone with reproducible material properties. Dynamic hip screws (DHS; Synthes, Paoli, PA) were inserted with the manufacturer's recommended instrumentation to a depth of 40 mm, yielding a 12.2 mm distance between the implant tip and the femoral head apex. To simulate a specific, nonideal, yet clinically acceptable implant placement, lag screws were inserted with 7 mm posterior offset parallel to the femoral neck axis.[22,23]

Implant shafts were rigidly mounted to a base fixture in a material test system at 149° to the horizontal plane (Fig. 1). For vertical loading of the femoral head, this implant orientation reflected a 130° femoral neck angle, a 16° resultant joint load vector, plus 3° offset of the femoral shaft axis from the sagittal plane. In this fixture, the back plate of the steel shell rested against a polyethylene support to simulate constraints characteristic for a reduced unstable pertrochanteric fracture at time of completion of implant sliding. Specifically, this support prevented lateral translation of the head-neck complex to represent a reduced fracture but allowed for varus collapse, as clinically observed in case of deficient posteromedial neck support and comminution (Fig. 1A).

The femoral head surrogates were confined in a 5-mm-thick, polished stainless-steel shell to allow for dynamic loading with a material test system (8874 Instron, Canton, MA). Compressive load cycles were applied to the steel shell over a horizontal bearing and polyethylene meniscus to ensure a purely vertical force vector, which consistently traced the superior aspect of the femoral head. Dynamic, sinusoidal loading was applied at 3 cycles per second up to 100,000 load cycles or until implant cutout, whichever occurred first. Of 12 identical specimens, 3 specimens were tested at each of 4 load levels (0.8 kN, 1.0 kN, 1.2 kN, and 1.4 kN) at a load ratio of 0.1 (ie, cyclic loading from 10% to 100% of load level).

Implant cutout was detected by means of electrical conductivity between the implant and the steel shell, which triggered an instantaneous stop of the test system to preserve the cutout stage. The number of load cycles to cutout failure (N_{CO}) was registered by the material test system. In addition, the 3-dimensional migration of the femoral head-neck complex in respect to the implant was continuously recorded with an electromagnetic motion tracking system (PcBird, Ascension Tech., Burlington, VT). From these motion data, femoral head migration was analyzed in terms of varus collapse (α_{varus}) and rotation around the neck axis (α_{neck}) and expressed as a function of the applied loading cycles (N).

Model Validation

To demonstrate how implant migration in surrogate specimens correlates to that in native bone, 11 nonembalmed human cadaveric femur specimens were tested in the above-described cutout model (Table 1). Dual-energy x-ray absorptiometry (DEXA) measurements were performed on all specimens to quantify bone mineral density (BMD) of the proximal femur. The combined BMD of the femoral neck, greater trochanter, and intertrochanteric region was expressed in terms of T scores. Specimens were stratified according to the World Health Organization into 3 groups, comprised of normal ($T > -1$), mildly osteoporotic ($-2.5 < T \leq -1$), and severely osteoporotic ($T \leq -2.5$) bone. Femoral necks were osteotomized

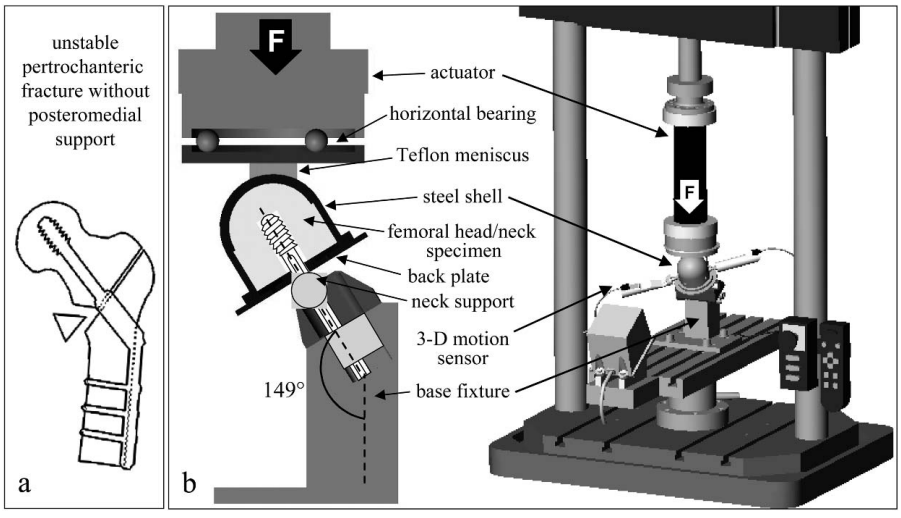

FIGURE 1. A, Fracture model (OTA 31-A.2) and (B) cutout simulator, shown in cross-sectional view and in assembly with material test system.

TABLE 1. DHS Cutout Simulation in Cadaveric Specimens Under 2.0 kN Cyclic Loading

Specimen No.	Gender	Side	Age (yrs)	T Score	Osteoporosis	Load Cycles	End Point
1	Female	R	71	−5.6	Severe	548	Cutout
2	Male	L	79	−2.7		82,752	Cutout
3	Male	R	81	−2.7		100,000	No cutout
4	Female	L	77	−2.0	Mild	91,995	Implant breakage
5	Female	L	85	−1.5		57,473	Implant breakage
6	Male	L	74	−1.3		4,539	Cutout
7	Female	L	75	−1.2		39,322	Cutout
8	Male	R	81	−0.9	Normal	93,236	Implant breakage
9	Male	R	82	−0.6		195	Cutout
10	Female	L	65	0.0		100,000	No cutout
11	Female	R	82	0.1		88	Cutout
Total	6 F, 5 M	5 R, 6 L	77.5 ± 5.8	−1.7 ± 1.6	NA	NA	6 cutout

Of 11 specimens, 6 failed by implant cutout, 2 sustained 100,000 load cycles, and 3 exhibited implant shaft breakage.
NA, not applicable; R, right; L, left.

perpendicular to the neck axis 50 mm from the apex of the head with a precision circular saw. Each femoral head was embedded into the 50-mm diameter stainless-steel shell with low-melting-point alloy and additionally secured against rotation with 3 set screws. Immediately after specimen potting, the steel shell was cooled with ice water to prevent thermal degeneration of the femoral head. Dynamic hip screw implants were inserted according the previously described technique, location, orientation, and depth. Specimens were mounted in the test setup and subjected to sinusoidal compression at a 2 kN load level and a load ratio of 0.1 (loading range 0.2 kN–2 kN) for 100,000 cycles or until cutout failure, whichever occurred first. For each specimen group, average migration histories (α_{varus}, α_{neck}) were computed to allow for direct comparison to the migration patterns observed in surrogate bone specimens.

Implant Evaluation

After correlation of the cutout behavior in surrogate specimens to that in cadaveric specimens of known bone quality, the cutout model was implemented to delineate differences in migration resistance among various implant designs. In the same manner as DHS implants, 3 additional implant designs were tested (Fig. 2): the helical blades of the dynamic helical hip system (DHHS; Synthes USA) and trochanteric fixation nail (TFN; Synthes USA) and the lag screw of the Gamma nail (Howmedica-Stryker-Osteonics, Rutherford, NJ). Implants were selected to represent principal differences in design (traditional thread [DHS, Gamma] vs. helical blade [DHHS, TFN]) and configuration (side plate devices [DHS, DHHS] versus intramedullary constructs [Gamma, TFN]), in which side replace devices have a smaller shaft diameter as compared with the intramedullary constructs tested. Each implant type was inserted into 12 surrogate foam specimens in accordance with the manufacturer's guidelines to the previously defined location. These 12 specimens per implant type underwent the identical test procedure as previously described for DHS testing in surrogate foam specimens. For each implant design at each load level, the average number of load cycles to cutout failure (N_{CO}) and the average migration histories (α_{varus}, α_{neck}) were assessed. To test the hypothesis that one implant design can provide significantly higher N_{CO} results than the remaining implant designs, analysis of variance of a statistical model was used, expressing $\log(N_{CO})$ as a function of load and type of implant:

$$\log(N_{CO}) = \beta_A + I_B\delta_B + I_c\delta_C + I_D\delta_D + \alpha$$

A represents the implant type with highest average N_{CO}. *B*, *C*, and *D* are the remaining implant types. β_A is the intercept for $\log(N_{CO})$ values of implant A. Intercepts corresponding to the remaining implants are $\beta_A + \delta_x$. I_x represents indicator variable 1 if the observation is from implant type x and 0 otherwise. α represents a common slope relating the increase in log cycles with the increase in load level. Before analysis of variance of $\log(N_{CO})$, a Kolmogorow-Smirnov test was conducted to ensure that residuals were not distinguishable from a normal distribution.

An additional statistical analysis was performed between those 2 implant designs that yielded the highest and second-highest average N_{CO} results. N_{CO} was ranked within the strata of load levels, and 10,000 randomizations of the ranked data set within a group were analyzed.

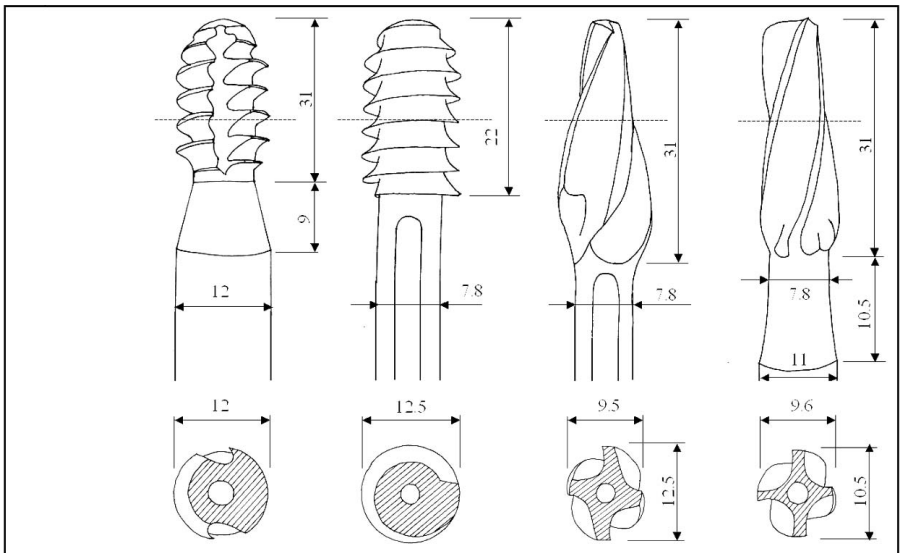

Implant	Gamma	DHS	DHHS	TFN
Design	screw	screw	blade	blade
Material	stainless steel	stainless steel	stainless steel	Titanium
Construct	intramedullary	side plate	side plate	intramedullary

FIGURE 2. Implant designs for testing of cutout resistance, shown in side view and as cross-section through the implant tip.

RESULTS

Dynamic hip screw cutout in surrogate foam specimens occurred by varus collapse and concomitant rotation of the femoral head around the neck axis. The average number of load cycles to cutout failure (N_{CO}) was 34107 ± 35418, 1136 ± 310, 96 ± 114, and 10 ± 5 for load amplitudes of 0.8 kN, 1.0 kN, 1.2 kN, and 1.4 kN, respectively. The cutout mechanism and cutout location were highly reproducible and correlated with clinically observed cutout failure, as well as with cutout in cadaveric specimens (Fig. 3).

Dynamic hip screw migration in surrogate specimens in terms of varus collapse α_{varus} and rotation of the femoral head around the neck, α_{neck}, was highly reproducible, as shown in Figure 4 for 3 specimens under 1 kN cyclic loading. Consistent in all tested specimens, the α_{neck} rotation of the femoral head around the implant resembled a motion corresponding to hip extension. Both α_{varus} and α_{neck} continuously progressed with an increase in loading cycles. The amount of migration per load cycles increased for increasing load amplitudes. After 1 load cycle, α_{varus} advanced to 3.7 ± 1.1°, 5.7 ± 1.1°, 10.5 ± 2.5°, and 16 ± 2.5° for load amplitudes of 0.8 kN, 1.0 kN, 1.2 kN, and 1.4 kN, respectively. After 1 load cycle, α_{neck} was 21.2 ± 7.5°, 26.1 ± 5.4°, 39.8 ± 4.7°, and 44.8 ± 1.8° for load amplitudes of 0.8 kN, 1.0 kN, 1.2 kN, and 1.4 kN, respectively. At cutout, α_{varus} and α_{neck} advanced on average to 26.5 ± 4.3° and 75 ± 12.6°, respectively, for the 12 DHS implants tested in surrogate specimens.

Model Validation

The 11 cadaveric specimens had an average T score of −1.7, ranging from 0.1 to −5.6 (Table 1). In cadaveric speci-

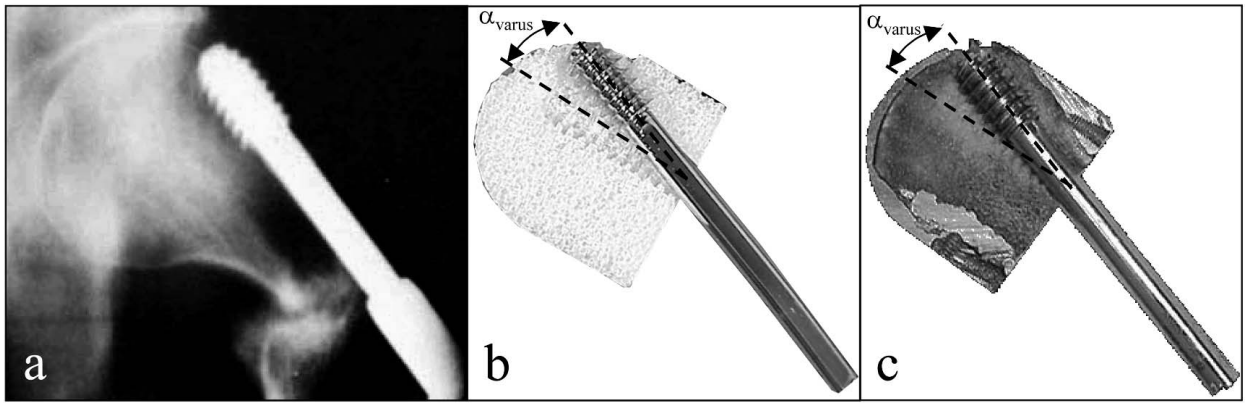

FIGURE 3. Dynamic hip screw cutout (A) on patient x-ray, (B) in surrogate foam, and (C) in cadaveric specimen.

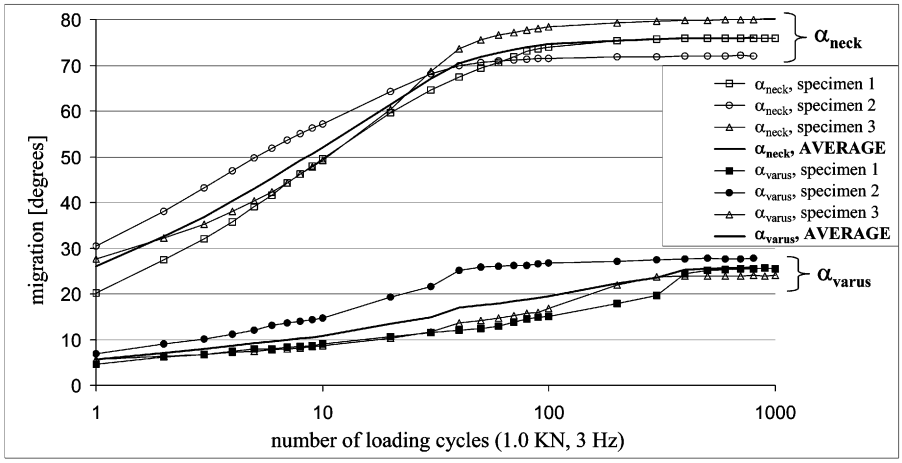

FIGURE 4. Dynamic hip screw migration in foam specimens at 1 KN: femoral head rotation around the implant shaft (α_{neck}) and into varus (α_{varus}).

mens subjected to 2 kN cyclic loading, DHS cutout failure occurred in 6 specimens (T = −1.9 ± 2.0) after 21241 ± 33788 load cycles. Two specimens sustained 100,000 load cycles without cutout. These specimens had T scores of 0 and −2.7. Three specimens exhibited lag screw fatigue fracture of the implant shaft after 57473, 91995, and 93236 load cycles.

Cutout occurred at a consistent location at α_{varus} and α_{neck} angles of 18 ± 5.2° and 77 ± 15.2°, respectively. However, corresponding migration histories greatly varied. After 10 loading cycles, α_{varus} ranged from 1.8° to 10°, and α_{neck} ranged from 0.8° to 60°. Complete migration histories of the 4 mildly osteoporotic specimens (T = −1.4 ± 0.4) are depicted in Figure 5 in comparison to the average migration history in surrogate specimens under 0.8 kN cyclic loading. Migration histories in these mildly osteoporotic specimens reasonably correlated to those obtained in surrogate specimens, but exhibited inferior reproducibility despite stratification for bone quality.

Implant Evaluation

The average numbers of load cycles to cutout failure (N_{CO}) for each of the 4 implant designs are summarized in Table 2. For statistical analysis with the log(N_{CO}) model, residuals were not distinguishable from a normal distribution using the Kolmogorov-Smirnov test. Analysis of variance confirmed that TFN implants sustained statistically significant

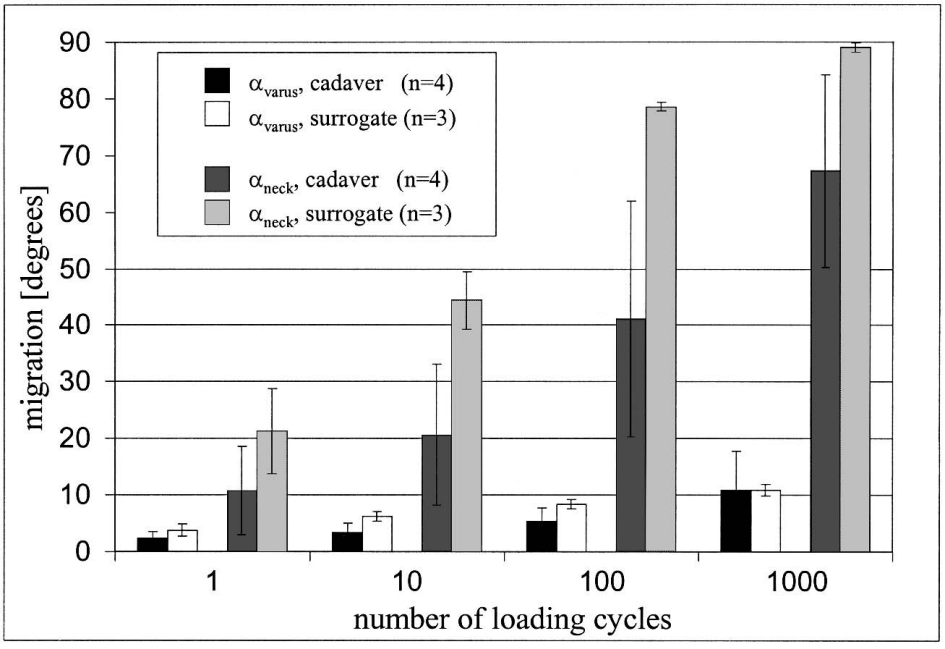

FIGURE 5. Comparison between DHS migration in surrogate foam specimens at 1 kN cyclic loading (n = 3) to migration in cadaveric specimens (mildly osteoporotic, n = 4) at 2 kN cyclic loading.

TABLE 2. Effect of Implant Design on Cutout Resistance. Summary of the Load Cycles Required to Induce Cutout Failure for 4 Specific Implant Designs, Tested at 4 Load Amplitudes up to a Maximum of 100,000 Load Cycles

Load Level	Specimen No.	Load Cycles			
		Gamma	DHS	DHHS	TFN
0.8 kN	1	57,287	11,182	100,000	Not tested
	2	100,000	16,240	100,000	Not tested
	3	100,000	74,900	100,000	Not tested
	Average		34,107		Not tested
1.0 kN	1	1222	1066	24,325	62,587
	2	815	866	100,000	42,852
	3	7580	1475	32,871	100,000
	Average	3206	1136		
1.2 kN	1	1197	53	10,934	28,030
	2	405	10	10,986	23,685
	3	1081	226	1635	33,165
	Average	894	96	7852	28,292
1.4 kN	1	403	7	250	237
	2	250	7	19	150
	3	1558	16	95	6875
	Average	737	10	121	2421

TFN implants were tested only at 3 load levels, because no cutout failure was anticipated at the lowest load amplitude (0.8 kN). If 100,000 loading cycles were completed without cutout, no group average was computed.

higher N_{CO} values as compared with DHS, DHHS, and Gamma implants, with the associated 1-tailed *P* values being 0.00005, 0.02, and 0.0003, respectively. The randomization test between the TFN and DHHS N_{CO} results yielded a probability of 0.0215 for a difference as large or larger than observed to occur.

Implant designs distinctively affected migration kinematics in terms of α_{varus} and α_{neck} (Fig. 6). After 100 cycles at 1 kN load amplitude, α_{varus} advanced to 1.4 ± 0.1°, 8 ± 1.6°, 12 ± 1.7°, and 20 ± 6.3° for the TFN, DHHS, Gamma, and DHS implants, respectively. After 100 loading cycles at 1 kN, α_{neck} advanced to 6 ± 0.8°, 26 ± 5.5°, 69 ± 2.8°, and 75 ± 3.5° for the TFN, DHHS, Gamma, and DHS implants, respectively.

DISCUSSION

Lag screw cutout is a multifactorial challenge, affected by bone strength, fracture pattern, quality of reduction, implant placement, and implant design. With the exception of implant design, these factors contributing to implant cutout are either difficult or impossible to control. Therefore, the aim of the present study was to establish a cutout model that was able to demonstrate significant differences in cutout resistance between specific implant designs.

A host of clinical and laboratory studies have attempted to identify implants with superior resistance to cutout failure.[10,15–18,20] In laboratory studies, fixation failure under static loading is reported to occur between 1800 N[20] and 6050 N[10] axial loading due to cutout or bending of the lag screw.[10,15,20] Haynes et al divided their specimens into a "hard bone" and "soft bone" group.[15] "Hard bone" specimens failed by lag screw bending at 4770N, and "soft bone" specimens exhibited cutout failure at 3117 N static loading. However, none of these studies was able to delineate statistically significant differences in cutout resistance between specific lag screw designs. After cutout testing of 4 lag screw designs in 48 cadaveric specimens yielded no significant differences in holding power, Jenny et al concluded in 1999 that it seems, therefore, unnecessary to advocate more sophisticated devices.[17] In contrary, Richards et al found significant differences between 2 implant designs under quasistatic loading conditions, but concluded that optimum shape and size of implants is still unknown and needs to be defined in laboratory tests.[24] Larsson et al were able to demonstrate statistically significant differences in implant migration between 3 different devices tested in cadaveric

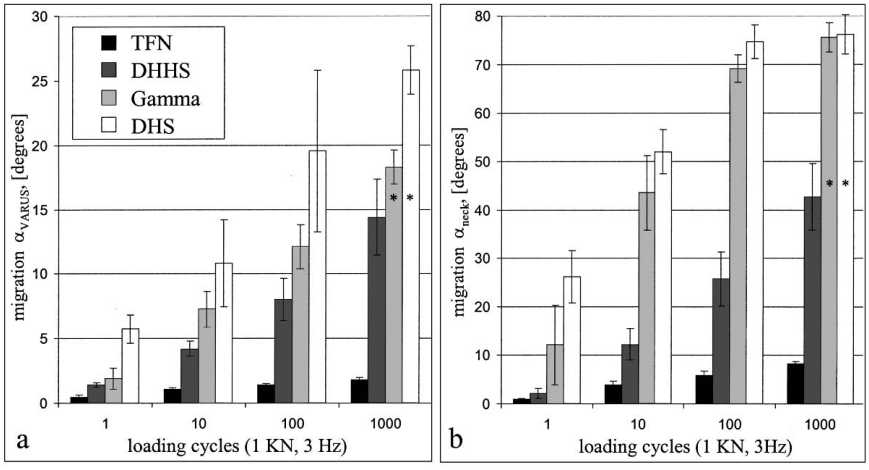

FIGURE 6. Implant specific migration into varus (A) and around implant shaft (B), shown for 4 implant types tested at 1 kN cyclic loading in surrogate foam specimens (n = 3 per implant). *One Gamma and 1 DHS implant failed by cutout after 815 and 866 cycles, respectively, and their migration values at cutout was included in the 1000 loading cycles column.

unstable pertrochanteric fractures under dynamic loading conditions.[19] However, specimens were only exercised up to 20,000 loading cycles, at which time only 5 out of 24 specimens sustained cutout failure. Most recently, Speitling et al simulated lag screw cutout in osteoporotic bone substitutes made of polyurethane foam to eliminate the complexity and variability of cadaveric specimens.[21] Under cyclical loading in an unstable fracture scenario, they successfully induced clinically observed cutout in a single implant design at load amplitudes of, on average, 1099 N.

Similar to Speitling et al, the presented model induced cutout under dynamic loading in defined polyurethane specimens and delivered in addition a direct correlation to implant cutout in cadaveric specimens. Furthermore, the present model simulates a specific lag screw insertion offset to account for a well-recognized clinical factor contributing to cutout failure by inducing rotational moments around the implant shaft.[22,23,25] Results, therefore, reflect implant cutout due to combined axial loads and rotational moments. Although prior studies determined the rotational stability of lag screw fixation constructs in response to quasistatic torsional loading,[13,26] the present model simulates for the first time cutout under combined axial and torsional loading.

The number of load cycles to cutout failure (N_{CO}) provides a direct comparison between migration resistances of implants tested under identical loading conditions. However, the absolute magnitude of N_{CO} is dependent on the loading history and specimen properties and may not, therefore, directly translate to implant fixation durability in vivo. Statistical comparison of N_{CO} was conducted using a log model and analysis of variance, assuming normally distributed residuals, even though data were truncated at 100,000 loading cycles. However, analyzing the data with the Kolmogorov-Smirnov test revealed that this assumption is a reasonable approximation. To further verify the statistical results, a randomization test of the 2 implants with the closest statistical results (ie, TFN versus DHHS) was conducted. In this test, data were ranked within the load level group, and 10,000 randomizations of the ranked data set within a group were analyzed. The 2-tailed probability of a difference as large or larger than that observed was 0.0215, corroborating results of the employed statistical model.

Next to the number of load cycles to cutout failure, implant migration tracking determined dramatic differences in the migration history between specific implant designs. For all implant designs, migration occurred by concomitant femoral head rotation into varus and rotation around the implant shaft. Blade-type implant designs significantly delayed the onset of this migration. However, upon migration onset, the amount of migration increased exponentially in all implants until cutout failure occurred. This observed delay in migration onset may clinically provide the opportunity for fracture healing before implant migration occurs. In contrast, if fixation failure and migration begin before fracture healing, results of this study suggest a continuous and rapid increase in fixation instability and subsequent implant cutout.

Dynamic hip screw cutout simulation in cadaveric specimens was complicated by large differences in T scores between specimens and by a poor correlation between T scores and N_{CO}. In 2 specimens, implant shaft bending instead of cutout occurred. Dynamic hip screw bending and breakage has been reported in other laboratory studies.[10,15,20] However, the incidence of implant breakage observed in laboratory studies may not represent the clinical scenario, in which bone healing and settling of the fracture enable load sharing, which gradually decreases forces to the lag screw. Cutout failure in cadaveric specimens required a higher load amplitude (2.0 kN) as compared with surrogate foam specimens (0.8 kN) for a comparable number of load cycles. This can be contributed to inferior constitutive properties of the polyurethane foam as compared with trabeculare bone and to the absence of a dense subchondral layer in the surrogate specimens. The reasonable correlation between implant migration histories in surrogate specimens and cadaveric specimens supports the validity of results obtained with surrogate specimens. Given the ease of availability, superior reproducibility, and cost considerations, surrogate specimens provide an attractive alternative to cutout simulation on cadaveric specimens.

The presented cutout model simulated a worst-case scenario by accounting for poor bone quality, an unstable fracture, dynamic loading, and implant offset. Albeit the simplified fracture pattern, loading regimen, and implant offset may not fully represent the clinical situation, potential methodological biases are not systematically in favor of any of the tested implants. This controlled and reproducible cutout model was capable of determining significant differences in cutout resistance between specific implant designs. Given the large geometric, constitutive, and configuration differences among contemporary implants for pertrochanteric fracture fixation, this cutout model provides a valuable tool to predict potential benefits of implant design parameters on implant fixation durability. The superior cutout resistance observed for the TFN implant suggests that this novel blade-type design may provide superior fixation strength in presence of osteoporotic bone and unstable fractures. Because it is more effective at supporting torsional loading, it may be more forgiving in case of imprecise implant placement. However, results of this study only describe implant performance in regard to cutout failure in absence of fracture healing and do not take into account alternative failure modes, such as lag screw jamming,[27] side plate pulloff,[15] iatrogenic fractures,[28] or fatigue fractures after implant removal.[29]

REFERENCES

1. Richmond J, Aharonoff GB, Zuckerman JD, et al. Mortality risk after hip fracture. *J Orthop Trauma*. 2003;17:53–56.

2. Clawson DK. Trochanteric fractures treated by the sliding screw plate fixation method. *J Trauma*. 1964;27:737–752.
3. Madsen JE, Naess L, Aune AK, et al. Dynamic hip screw with trochanteric stabilizing plate in the treatment of unstable proximal femoral fractures: a comparative study with the Gamma nail and compression hip screw. *J Orthop Trauma*. 1998;12:241–248.
4. Rao JP, Banzon MT, Weiss AB, et al. Treatment of unstable intertrochanteric fractures with anatomic reduction and compression hip screw fixation. *Clin Orthop*. 1983;175:65–71.
5. Laros GS. The role of osteoporosis in intertrochanteric fractures. *Orthop Clin North Am*. 1980;11:525–537.
6. Baumgaertner MR, Curtin SL, Lindskog DM, et al. The value of the tip-apex distance in predicting failure of fixation of peritrochanteric fractures of the hip. *J Bone Joint Surg Am*. 1995;77:1058–1064.
7. Yoshimine F, Latta LL, Milne EL. Sliding characteristics of compression hip screws in the intertrochanteric fracture: a clinical study. *J Orthop Trauma*. 1993;7:348–353.
8. Davis TR, Sher JL, Horsman A, et al. Intertrochanteric femoral fractures. Mechanical failure after internal fixation. *J Bone Joint Surg Br*. 1990;72: 26–31.
9. Parker MJ. Cutting-out of the dynamic hip screw related to its position. *J Bone Joint Surg Br*. 1992;74:625.
10. Wu CC, Shih CH, Lee MY, et al. Biomechanical analysis of location of lag screw of a dynamic hip screw in treatment of unstable intertrochanteric fracture. *J Trauma*. 1996;41:699–702.
11. Jacobs RR, McClain O, Armstrong HJ. Internal fixation of intertrochanteric hip fractures: a clinical and biomechanical study. *Clin Orthop*. 1980; 146:62–70.
12. Mainds CC, Newman RJ. Implant failures in patients with proximal fractures of the femur treated with a sliding screw device. *Injury*. 1989;20: 98–100.
13. Goldhagen PR, O'Connor DR, Schwarze D, et al. A prospective comparative study of the compression hip screw and the gamma nail. *J Orthop Trauma*. 1994;8:367–372.
14. Parker MJ, Blundell C. Choice of implant for internal fixation of femoral neck fractures. Meta-analysis of 25 randomized trials including 4,925 patients. *Acta Orthop Scand*. 1998;69:138–143.
15. Haynes RC, Pöll RG, Miles AW, et al. An experimental study of the failure modes of the Gamma locking nail and AO dynamic hip screw under static loading: a cadaveric study. *Med Eng Phys*. 1997;19:446–453.
16. Haynes RC, Pöll RG, Miles AW, et al. Failure of femoral head fixation: a cadaveric analysis of lag screw cut-out with the gamma locking nail and AO dynamic hip screw. *Injury*. 1997;28:337–341.
17. Jenny JY, Rapp E, Cordey J. Type of screw does not influence holding power in the femoral head: a cadaver study with shearing test. *Acta Orthop Scand*. 1999;70:435–438.
18. Kauffman JI, Simon JA, Kummer FJ, et al. Internal fixation of femoral neck fractures with posterior comminution: a biomechanical study. *J Orthop Trauma*. 1999;13:155–159.
19. Larsson S, Elloy M, Hansson LI. Fixation of unstable trochanteric hip fractures. A cadaver study comparing three different devices. *Acta Orthop Scand*. 1988;59:658–663.
20. Meislin RJ, Zuckerman JD, Kummer FJ, et al. A biomechanical analysis of the sliding hip screw: the question of plate angle. *J Orthop Trauma*. 1990;4:130–136.
21. Speitling A, Schbettler R, Tschoeke SK, et al. Method for evaluation of hip screws cut-out behavior. *Osteosynthese Intl*. 2000;8:135–136.
22. Den Hartog BD, Bartal E, Cooke F. Treatment of the unstable intertrochanteric fracture. Effect of the placement of the screw, its angle of insertion and osteotomy. *J Bone Joint Surg Am*. 1991;73:726–733.
23. Kawaguchi S, Sawada K, Nabeta Y. Cutting-out of the lag screw after internal fixation with the Asiatic gamma nail. *Injury*. 1998;29: 47–53.
24. Richards RH, Evans G, Egan J, et al. The AO dynamic hip screw and the Pugh sliding nail in femoral head fixation. *J Bone Joint Surg Br*. 1990;72: 794–796.
25. Mohan R, Karthikeyan R, Sonanis SV. Dynamic hip screw: does side make a difference? Effects of clockwise torque on right and left DHS. *Injury*. 2000;31:697–699.
26. Goodman SB, Davidson JA, Locke L, et al. A biomechanical study of two methods of internal fixation of unstable fractures of the femoral neck. A preliminary study. *J Orthop Trauma*. 1992;6:66–72.
27. Kyle RF, Wright TM, Burstein AH. Biomechanical analysis of the sliding characteristics of compression hip screws. *J Bone Joint Surg Am*. 1980; 62:1308–1314.
28. Lacroix H, Arwert H, Snijders CJ, et al. Prevention of fracture at the distal locking site of the gamma nail. A biomechanical study. *J Bone Joint Surg Br*. 1995;77:274–276.
29. Kukla C, Pichl W, Prokesch R, et al. Femoral neck fracture after removal of the standard gamma interlocking nail: a cadaveric study to determine factors influencing the biomechanical properties of the proximal femur. *J Biomech*. 2001;34:1519–1526.